Geomorphology 368 (2020) 107349

Contents lists available at ScienceDirect

Geomorphology

journal homepage: www.elsevier.com/locate/geomorph

Runoff and soil moisture as driving factors in suspended sediment transport of a small mid-mountain Mediterranean catchment

Josep Fortesa [a,b,*], Jérôme Latron [c], Julián García-Comendador [a,b], Jaume Company [a,b], Joan Estrany [a,b]

[a] Mediterranean Ecogeomorphological and Hydrological Connectivity Research Team, Department of Geography, University of the Balearic Islands, Ctra. Valldemossa km 7.5, 07122 Palma, Balearic Islands, Spain
[b] Institute of Agro-Environmental and Water Economy Research-Inagea, University of the Balearic Islands, Ctra. Valldemossa km 7.5, 07122 Palma, Balearic Islands, Spain
[c] Institute of Environmental Assessment and Water Research (IDAEA), Spanish Research Council (CSIC), Jordi Girona 18, 08034 Barcelona, Spain

ARTICLE INFO

Article history:
Received 1 May 2020
Received in revised form 10 July 2020
Accepted 10 July 2020
Available online 18 July 2020

Keywords:
Suspended sediment transport
Soil moisture conditions
Hysteretic patterns
Mediterranean catchment

ABSTRACT

Soil moisture conditions play a key role in runoff and sediment load dynamics in river catchments of contrasting ecosystems. However, the highly marked seasonality of Mediterranean climate affects hydrological processes and sediment transport strongly, as evapotranspiration determines a succession of wet, transition and dry periods throughout a hydrological year. This study examines results of soil moisture, water and sediment fluxes during five hydrological years in a representative small mid-mountain Mediterranean catchment. It aims to assess the sediment load contribution and its variability at different temporal scales. Precipitation, runoff and suspended sediment load were calculated at annual, seasonal and event scales to assess inter- and intra-annual variability. A database with 45 events was used to identify the main controlling factors over sediment load thought bivariate relationships and an analysis of soil moisture-discharge and discharge-suspended sediment concentration hysteresis. At the annual scale, lithology, land use and soil conservation structures characteristic of the catchment caused low values of sediment yield, although inter-annual rates varied by up to three orders of magnitude (0.08 to 11.86 t km^{-2} y^{-1}). Seasonal analysis of accumulated sediment load showed that 80% was generated during the autumn and winter seasons. At the event scale, streamflow and soil moisture were the controlling factors for the largest sediment load contributions. The highest frequency of clockwise discharge-suspended sediment concentration hysteresis revealed that most of the sediment was generated from nearby sources, although the largest sediment loads were contributed under wet antecedent conditions, as depicted by the soil moisture-discharge hysteresis assessment.

1. Introduction

Mediterranean landscapes are complex because of the local variations in topography, soils and surface water, which cause a lot of spatial variability in soil depth, infiltration capacity, slope gradient and land use characteristics (Geeson et al., 2002). As a result, Mediterranean catchments are characterized by a wide diversity of hydrological regimes (Oueslati et al., 2015) controlling sediment transport (Jaeger et al., 2017). These regimes that have been modified during millennia through deforestation, terracing and irrigation schemes, have seen intensified change in recent decades with urban development, dam construction, channelling of water, land abandonment, afforestation and reforestation (Hooke, 2006). In this physical context, an increase in soil water content promotes favourable conditions for runoff (hereinafter R) and sediment load (hereinafter SL), because this context affects infiltration capacity, soil water storage and especially soil moisture, which regulate runoff generation processes more than rainfall (Seeger et al., 2004). R in Mediterranean catchments may be caused by both Hortonian and saturation processes, as the dominant processes may change with the seasons (Kirkby, 2005). Although both mechanisms can co-exist within a catchment, they are affected by soil moisture conditions enabling greater hydrological response and sediment transport (Lana-Renault et al., 2007; Estrany et al., 2009). Favourable soil moisture (hereinafter SM) conditions occur during periods of maximum soil moisture content, which may change from year to year depending on annual rainfall distribution. Flood events outside this soil moisture window tend to generate smaller R and SL contributions than events within the soil moisture window because the former occurs under conditions of lower moisture or relatively dry soil (Gómez et al., 2014). Antecedent moisture conditions were evaluated by direct measurements, such as monitoring soil moisture at the catchment scale (Seeger et al., 2004; Favaro and Lamoureux, 2014; Pulley and Collins, 2019). Catchment SM modelling (Bussi et al., 2014; Gómez et al., 2014), antecedent

* Corresponding author at: Institute of Agro-Environmental and Water Economy Research-Inagea, University of the Balearic Islands, Ctra. Valldemossa km 7.5, 07122 Palma, Balearic Islands, Spain.
E-mail address: josep.fortesa@uib.cat (J. Fortesa).

https://doi.org/10.1016/j.geomorph.2020.107349

discharge or antecedent precipitation are also used as indirect measurements of soil moisture conditions in non-Mediterranean catchments (Palleiro et al., 2014; Rodríguez-Blanco et al., 2019) and Mediterranean ones (Giménez et al., 2012; Taguas et al., 2013; Fortesa et al., 2020a). Nevertheless, representative measurements of SM at the catchment scale are still difficult to obtain because of the high spatial and temporal variability and multiple factors relating to SM (i.e., soil texture, topography, precipitation and vegetation; Zucco et al., 2014; Korres et al., 2015). Although spatial optimization of the SM network reduces the number of sampling points, monitoring difficulties leads to the use of previously reported indirect measurements, which are easier to obtain and monitor (Brocca et al., 2010). Penna et al. (2011) assessed the role of SM in R generation in a small alpine headwater catchment, showing through hysteretic loop direction how the timing of peaking between SM and R identified wetness conditions prior to a flood event. The highest sediment yields (hereinafter SY) in Europe were found in Mediterranean and mountainous regions where more than 50% of records exceeded 200 t km^{-2} yr^{-1} (Vanmaercke et al., 2011) due to a combination of physical and anthropogenic factors. Consequently, case studies of the role of soil moisture in runoff and sediment generation in Mediterranean catchments are needed to verify the data obtained by indirect measurements, modelling and remote sensing (Huza et al., 2014; Uber et al., 2018).

The aim of this paper is to assess the role of SM in SL and its variability at the annual, seasonal and event scales over a 5-year period in the Es Fangar Creek (3.4 km^2; Mallorca, Spain), a representative small mid-mountain Mediterranean catchment. Rainfall, soil moisture, runoff and suspended sediment were evaluated through the analyses of several variables. Soil moisture-discharge and discharge-suspended sediment hysteresis at the event scale were carried used to determine the factors controlling sediment load. The understanding of SL contributions requires a prior understanding of SM changes, because moisture conditions control hydrological processes and sediment transport directly.

2. Study area

Es Fangar Creek catchment (3.4 km^2) is a headwater tributary of the Sant Miquel River catchment (151 km^2) in the north of Mallorca Island (Fig. 1a, b and c). The lithology in the upper parts of the catchment consists mainly of massive calcareous and dolomite materials from the lower Jurassic (Lias) and dolomite and marl formations from the Triassic period (Rhaetian). In the valley bottoms, marl and marl-limestone formations from the middle-upper Jurassic (Dogger-Malm) and Cretaceous periods are dominant (Fig. 1d). Elevations range from 72 m.a.s.l. to 404 m.a.s.l. The mean slope of the catchment is 26% and the length of the main channel is 3.1 km (average slope of 22%). The drainage network is natural at the headwaters, although at the valley bottom the main stream was straightened and diverted in the past, with its banks fixed with dry-stone walls. In floodplain areas, check-dam terraces were also built in the past to control floods and prevent erosion (Fig. 1d and e). The terraces conserve agricultural soils, which have been identified as the main sediment source in the Es Fangar catchment. Subsurface tile drains were also installed to facilitate drainage during wet periods, hindering soil saturation and allowing agricultural activity. Soil and water conservation structures affect 16% of the catchment, supported by 32.4 km of dry-stone walls. Gradual abandonment of farmland in marginal areas has led to afforestation since 1950. Land uses in 1956 consisted of by rain-fed herbaceous crops (54%), forest (31%) and scrubland (15%). Today, the main land uses (Fig. 1e) are forest (63%, mainly located at the headwaters), rain-fed herbaceous crops (32%) and scrubland (5%). The consolidation of this forest transition means that 54% of the terraced land is currently covered by forest (Fig. 1e). The climate is classified on the Emberger scale (Guijarro, 1986) as Mediterranean temperate sub-humid. Mean annual rainfall (1964–2017, Biniatró AEMET station; see Fig. 1c) was 927 mm y^{-1} with a variation coefficient of 23% and a mean annual temperature of 15.7 °C. Rainfall of 180 mm in 24 h is calculated to have a recurrence period of 25 years (YACU, 2002). Mean annual runoff was 87 mm and the mean number of days with flow was 171 days during the hydrological years 2012–2017. In Es Fangar, the hydrological regime is classified as intermittent-flashy (Fortesa et al., 2020b).

3. Material and methods

3.1. Monitoring and data acquisition

Daily rainfall data have been obtained since 2012 from the B696 Biniatró AEMET station (Fig. 1e; 1 km from the catchment). In October 2014, a meteorological station was installed at Míner Gran (560 m.a.s.l.). This was more representative of the rainfall dynamics of Es Fangar headwaters. It was installed 1 m above the ground and connected to a HOBO Pendant® G Data Logger - UA-004-64 that recorded precipitation at 0.2 mm resolution. Linear regression was established ($n = 978$; R^2: 0.88) for daily rainfall (2014–2017) between the Biniatró and Míner Gran stations to reconstruct rainfall data series from 2012 to 2014 for the Míner Gran station.

The gauging station of Es Fangar Creek was constructed in July 2012. The cross-section has a rectangular broad-crested weir for low water stages, which measures low flows well (see Fig. 1f). A *Campbell Scientific CR200X* data logger measures the water stage continuously by a Campbell CS451 pressure sensor, and measures turbidity by an OBS-3+ turbidimeter with a double measurement range of 0–1000/1000–4000 NTU. In October 2014, a Water Content Reflectometer (Campbell Scientific CS625) was installed in a rain-fed herbaceous crop, 3 m from the gauge station. This provides continuous SM information at 0–30 cm depth. The SM measurements are assumed to be representative of those at the valley bottom (i.e., 32% of the catchment area). The deep soils of this area (Fig. 1d) show high field capacity, which allows the maintenance of an intermittent fluvial regime (i.e. 49% zero flow days). The datalogger takes readings every minute and records average readings every 15 min. Between 2012 and 2017, 17 direct flow velocity measurements were taken during baseflow conditions and flood events with a Q range between 0.004 and 2.166 m^3 s^{-1}, by using means of an OTT MF Pro electromagnetic water flow meter. These flow velocity measurements were used to establish the stage-discharge relationship. In addition, samples were collected with a rising-stage sampler modified from Schick (1967) and manually during storm events and baseflow periods. Samples (250 ml) were filtered with 0.45 μm filters, which were subsequently dried at room temperature and weighed on high-precision scales (i.e. 0.0001 g) to determine suspended sediment concentrations (hereinafter SSCs). Finally, SSCs derived from these samples were used to calibrate the turbidity probe in a range of 0.4 to 860 mg l^{-1} ($n = 38$; $R^2 = 0.81$).

3.2. Rainfall - soil moisture – runoff - suspended sediment assessment

Precipitation (P), runoff (R) and suspended sediment load (SL) were calculated at annual, seasonal, and event scales from continuous records of P, Q and SSC during 5 hydrological years (2012–17) to assess their temporal dynamics. SM was also used with the same aim but only covering three hydrological years (2014–2017). The SL was normalized to catchment area to obtain the SY.

3.2.1. Flood events analysis

A database of 45 flood events was generated with data for P, SM, Q and SS. A hydrological event was defined as when Q exceeded 0.036 m^3 s^{-1} (i.e. when water stage overflowed baseflow section). P-R-SSC were assessed with the 45 events. P-SM-Q-SSC were assessed with 28 events. The variables are summarized in Table 1 as (a) antecedent conditions and (b) event conditions. Antecedent conditions refer to antecedent precipitation (1 and 3 days), whereas event conditions refer to P, SM, Q, SS variables and the Normalized Soil Moisture Lag Time (hereinafter

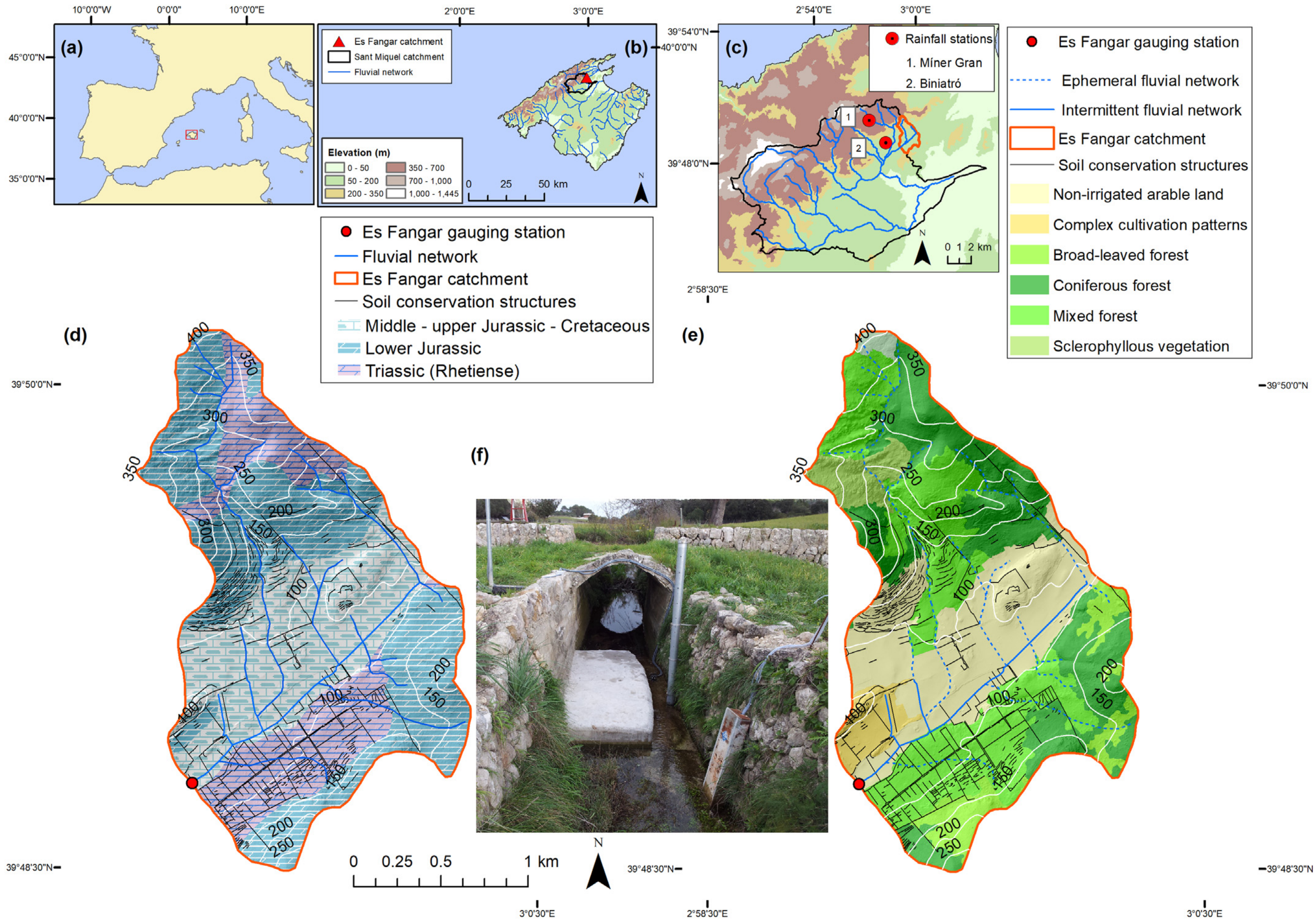

Fig. 1. Maps showing (a) the location of Mallorca in the Western Mediterranean Sea and (b) the location of Sant Miquel and Es Fangar catchments within the island. (c) Map of the Sant Miquel River catchment with the location of rainfall stations used in this study. (d) Geological and (e) land use maps of the Es Fangar catchment, showing the fluvial network and the locations of soil conservation structures and of the gauging station. (f) Upstream view of the cross-section at Es Fangar gauging station.

NSMLT). This last variable was computed as the time lag between storm onset and soil moisture peak, normalized by dividing by the duration of the rainfall event.

Bivariate statistical regressions were used to establish correlations between variables from Table 1. These equations were used descriptively for the P-R-SS-SM assessment. In order to identify the main factors driving SS transport, multiple relationships were calculated to investigate the influence of R and SL on $IP_{max}30$, Q_{max}, NSMLT and SM_{av}.

The catchment response under different SM conditions was also analysed. The values of R, Q_{max} and SL were used to create groups for upper and lower Q50 and Q75 of average SM. The same grouping was created for the upper and lower Q50 values of NSMLT, in order to assess the timing of the SM peak in relation to SL contributions. The Mann-Whitney test was applied to check whether significant differences (i.e. $p < 0.01$) between groups were due to different degrees of SM average or NSMLT.

Table 1
Variables of antecedent and event conditions selected to analyse the soil moisture-rainfall-runoff-suspended sediment relationships.

Antecedent conditions		Event conditions	
AP1d	Antecedent precipitation 1 day before (mm)	P_{tot}	Total precipitation (mm)
AP3d	Antecedent precipitation 3 days before (mm)	$IP_{max}30$	Maximum 30′ rainfall intensity (mm h^{-1})
		R	Runoff (mm)
		R_c	Runoff coefficient (%)
		Q_{max}	Peak discharge (m^3 s^{-1})
		SSC_{max}	Maximum suspended sediment concentration (mg l^{-1})
		SSC_m	Mean suspended sediment concentration (mg l^{-1})
		SL	Sediment load (t)
		NSMLT	Normalized Soil Moisture Lag Time
		SM_{av}	Soil moisture average (%)

3.2.2. Hysteresis analysis

The spatio-temporal relationships between SM, Q and SSC were analysed by a double hysteresis analysis. The first hysteresis analysis focused on the relationship between Q and SSC, using the hysteresis classification reported by Williams (1989). Hysteretic loops were accordingly classified as single line (i.e., Q and SS peaks are at the same time), a clockwise loop (i.e., SS peaks earlier than Q peak), a counter-clockwise loop (i.e., SS peaks later than Q peak) and complex (i.e., clockwise and counter-clockwise combination). The second hysteretic analysis assessed the condition preceding of the R event. As a result, an analysis of SM – Q hysteretic loops, following the method by Penna et al. (2011), was used to identify dry or wet antecedent conditions. During dry conditions, Q peaked before SM, leading to a clockwise hysteretic loop. During wet conditions, a counter-clockwise loop is seen when SM peaks earlier than Q. To investigate hysteretic patterns, R and SS contributions were analysed by hysteresis type for Q-SSC and SM-Q.

4. Results

4.1. Hydrological response and suspended sediment transport

4.1.1. Annual to seasonal scale

The mean annual P (840.8 mm $y^{-1} \pm 213$ mm y^{-1}) recorded during the five hydrological years was representative (−9%) of the long-term (1964–2017) annual rainfall (927 mm $y^{-1} \pm 215$ mm y^{-1}), but showed a high degree of variation (25% of variation coefficient, from 553 mm y^{-1} to 1090 mm y^{-1}). Positive linear relationships were observed between annual P, R and SL ($R^2 \geq 0.90$, data not shown). Annual R ranged from 16.1 mm to 139.2 mm (mean value = 87.3 mm); SL contribution, from 0.3 t to 39.7 t y^{-1} (mean value = 18 t y^{-1}); and SY, from 0.08 to 11.86 t km^{-2} y^{-1} (mean value = 5.38 t km^{-2} y^{-1}).

Due to the inter- and intra-annual rainfall variability, contrasted amounts of R and SL were observed during the five years of the study period (Fig. 2). The general behaviour of R and SL dynamics throughout the hydrological year illustrated how, until late autumn-beginning of winter (i.e. 15–20% of the time), R and SL accounted for <20% of the annual amount. Although autumn had the widest range (11 to 42%) of SM values, the median SM was higher than in spring and summer (Fig. 1 Appendix). During winter and early spring (i.e., 30% to 50% of the time), R and SL accounted for an average of 77% and 76% respectively, with 52% of the accumulated P. In winter, the highest maximum, median and minimum values of SM were recorded (Fig. 1 Appendix).

Table 2
Largest runoff and sediment load values at the event scale for each hydrological year, and their relative contribution in each hydrological year and in the entire study period. The hydrological years 2013–14 and 2014–15 show two events because the maximum runoff and sediment load contributions occurred in different events: the maximum of each variable is in bold.

Hydrological year	Season of the event	Relative contribution Hydrological year (%)		Relative contribution Study period (%)	
		Runoff	Sediment load	Runoff	Sediment load
2012–13	Winter	20.8	43.1	3.1	1.1
2013–14	Autumn	**35.0**	6.9	5.4	1.2
	Summer	6.6	**77.1**	1.0	12.8
2014–15	Winter	28.9	20.5	**9.4**	9.0
	Winter	12.8	49.5	4.2	**21.8**
2015–16	Spring	14.9	47.8	0.6	0.1
2016–17	Winter	20.7	37.4	6.9	13.6

From mid-spring and summer (i.e., after 60% of the time), a dry period was established when P, R and SL averaged <17%, 4% and 18%, respectively. At the end of this dry period, large amounts of SL (i.e., 77% of annual yield) appear in the short term (i.e., 0.5% of the hydrological year), as occurred in the last month of the 2013–14 hydrological year (Fig. 2c) (Table 2).

Accordingly, the largest increases of cumulative R and SL in a short period of time were related to specific flood events. The largest R and SL during events were generated in winter, although SL contributions were more varied than R.

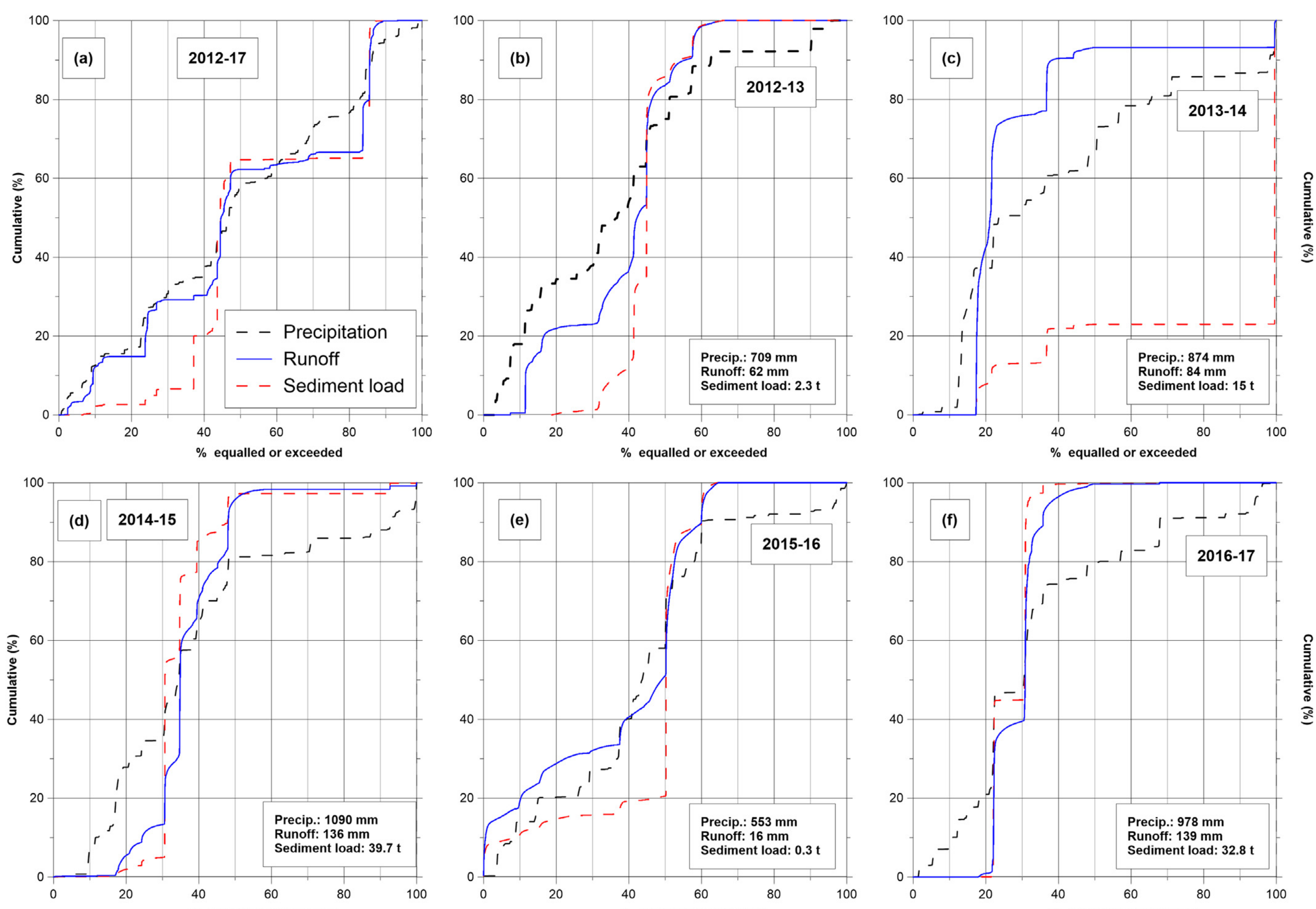

Fig. 2. Cumulative precipitation (mm), runoff (mm) and sediment load (t): (a) during the 5-year study period and (b to f) during each hydrological year.

4.1.2. Event scale

4.1.2.1. Hydro-sedimentary response. The 45 flood events recorded in the 2012–2017 hydrological period were analysed for the SL contributions at the event scale. The Q75 of the SL (corresponding to 1 t contribution) was exceeded in 12 events (27%). The SL exported during these events accounted for 91% of the total SL, although 73% was generated in only 5 events (Fig. 2 Appendix).

To identify those factors explaining SL variability at the event scale, seasonal relationships between P, R, Q_{max}, average SM and SL were evaluated (Fig. 3). The relationship between P and SL (Fig. 3a) was highly scattered and showed no significant correlation between variables, as SL contributions >1 t were generated with P amounts from 10 to 100 mm. However, autumn and winter correlations increased to R^2: 058 and R^2: 0.46, respectively. In these seasons, P events >50 mm generated SL > 1 t. In summer, P amounts between 30 and 40 mm generated varying SL contributions of 3 different orders of magnitude (i.e., 0.1 to 10 t).

Streamflow variables (R and Q_{max}) showed the closest correlations with SL (Fig. 3b and c). The R-SL relationship explained 67% of variance (Fig. 3b), increasing for autumn (R^2: 0.72) and winter (R^2: 0.77) events. Accordingly, the largest runoff events (*R* > 10 mm; SL > 0.4 t) occurred mainly in winter and autumn. The Q_{max}-SL relationship illustrated the closest correlation, with little variability between seasons. Events with $Q_{max} > 1\ m^3\ s^{-1}$ generated SL between 0.4 and 19.7 t.

The average SM during flood events explained 45% of variance (Fig. 3d). Events with $SM_{av} > 44\%$ (only in autumn and winter) generated SL contributions >0.8 t. The SM_{av}-SL correlation increased in autumn (R^2: 0.77) and winter (R^2: 0.75), in a similar way to R patterns. On the contrary, the SM_{av}-SL relationship for spring and summer events was much more scattered (Fig. 3d).

To analyse in detail the SS contribution at the event scale, $IP_{max}30$, Q_{max}, NSMLT and SM_{av} were added to the R-SL correlation (Fig. 4). $IP_{max}30$ (Fig. 4a) did not have a large influence on the SL, as events with P intensities ≈ 30 mm h^{-1} generated SL ranging from 0.1 to 10 t. However, P intensities >40 mm h^{-1} led to SL > 1 t. The combined analysis of R and Q_{max} illustrates how high values of these two variables gave the highest SL contributions. Events with *R* > 5 mm and $Q_{max} > 0.8\ m^3\ s^{-1}$ systematically resulted in SL ≥ 1 t (Fig. 4b). Use of NSMLT as the driving factor (Fig. 4c) made clear that higher values of NSMLT were related to low R and SL and vice versa. Thus, high R and SL contributions could be generated with low NSMLT values. A further assessment of this relationship was developed by using values of R, Q_{max} and SL for the upper and lower Q50 values of NSMLT. These parameters were compared and assessed with the Mann-Whitney test. Significant

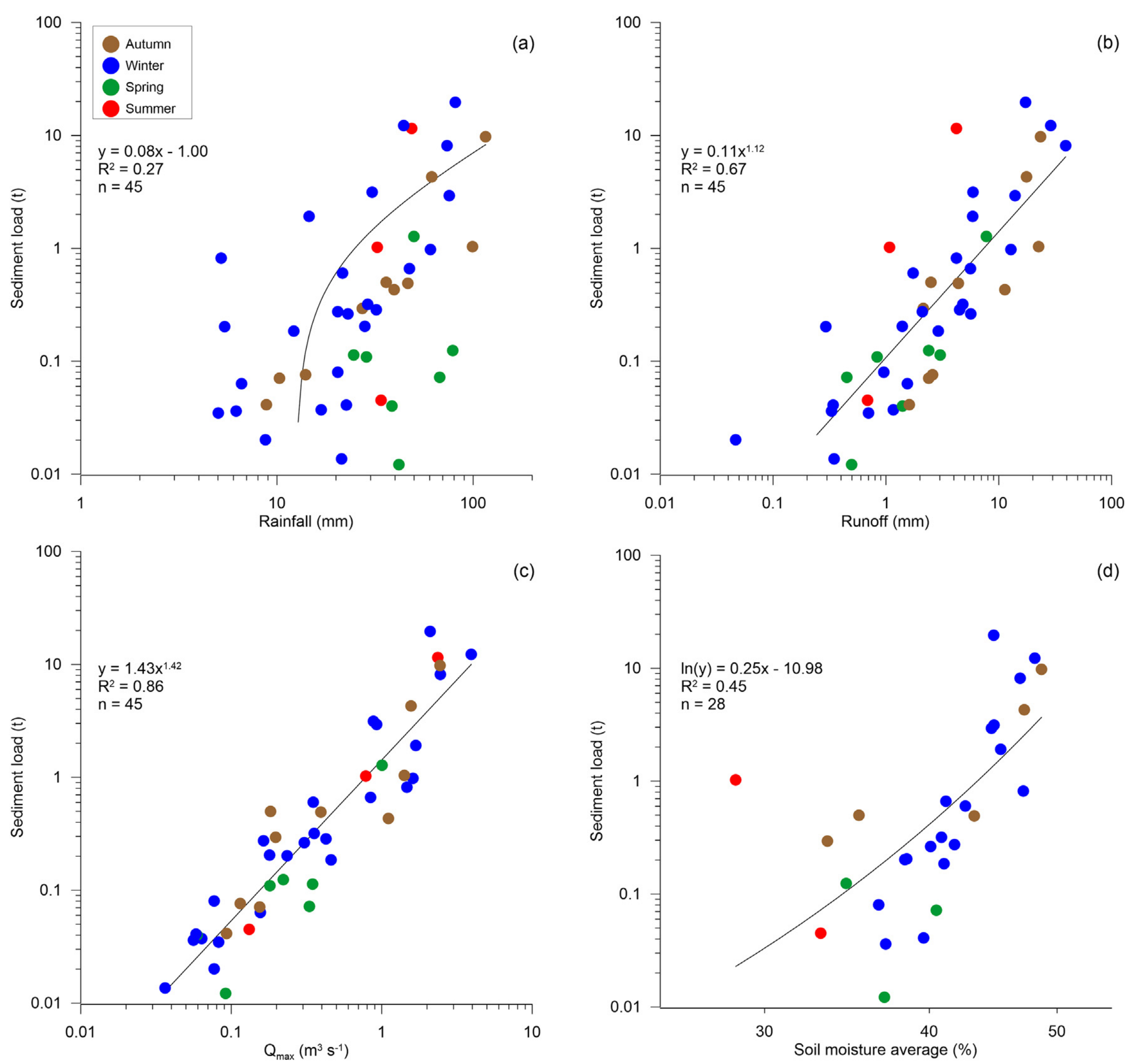

Fig. 3. Relationships at the event scale between (a) rainfall, (b) runoff, (c) maximum discharge and (d) soil moisture average with sediment load. Events are classified by seasons. Black lines show significant (*p* < 0.01) fits with their respective functions.

differences ($p < 0.01$) between upper and lower Q50 in the three variables were observed; i.e., NSMLT values < Q50 promoted higher values of R, Q_{max} and SL.

The average SM was also a good indicator for those events able to transport a larger amount of SL. Eight out of 9 events with SL > 1 t resulted in SM_{av} > 45% (Fig. 4d). The rest of the events with SL > 1 t occurred in summer (SM_{av}: 29%) with an intermediate P intensity (19.6 mm h^{-1}).

To analyse the role of SM_{av} in R, Q_{max} and SL, event groups based on upper and lower SM_{av} Q50 and Q75 were defined. For each group, the average, median and standard deviations of R, Q_{max} and SL were calculated. R, Q_{max} and SL were always significantly (according to the Mann-Whitney test; $p < 0.01$) higher for events with SM_{av} > Q50 (or SM_{av} > Q75) than for events with SM_{av} < Q50 (or SM_{av} < Q75) (Table 3). In addition, R, Q_{max} and SL increased from SM_{av} > Q50 to SM_{av} > Q75.

4.1.2.2. Discharge-suspended sediment concentration and soil moisture-discharge hysteretic patterns. Different sediment sources were activated throughout the year according to changing (linear, clockwise, counter-clockwise and complex) hysteresis patterns of Q-SSC (Table 4). The percentage distributions of linear, clockwise, counter-clockwise and complex hysteresis were 16%, 58%, 18% and 9%, respectively. In all seasons, clockwise loop behaviour was predominant, but especially during winter (31% of hysteresis). Complex hysteresis was not generated during spring and summer. The main R and SL contributions corresponded to clockwise (R: 57%, SL: 52%) and counter-clockwise (R: 18%, SL: 31%) hysteresis (Table 4).

Table 3
Average, median and standard deviation of runoff, Q_{max} and sediment load, considering alternatively all events, events based on upper and lower SM_{av} Q50 and events based on upper and lower SM_{av} Q75.

	Runoff	Q_{max}	SL		Runoff	Q_{max}	SL
	mm	$m^3 s^{-1}$	t		mm	$m^3 s^{-1}$	t
Average				Average			
All events	6.8	0.80	2.4	All events	6.8	0.80	2.4
SM_{av} < Q50	1.7	0.23	0.2	SM_{av} < Q75	2.6	0.31	0.4
SM_{av} > Q50	12.4	1.40	4.7	SM_{av} > Q75	17.8	2.07	7.5
Median				Median			
All events	2.5	0.35	0.4	All events	2.5	0.35	0.4
SM_{av} < Q50	1.1	0.20	0.2	SM_{av} < Q75	1.7	0.22	0.2
SM_{av} > Q50	5.9	1.19	2.4	SM_{av} > Q75	17.4	1.89	6.2
SD				SD			
All events	9.6	0.95	4.6	All events	9.6	0.95	4.6
SM_{av} < Q50	1.6	0.18	0.3	SM_{av} < Q75	3.1	0.25	0.7
SM_{av} > Q50	11.6	1.06	5.8	SM_{av} > Q75	12.4	0.92	6.3

SM – Q hysteresis revealed that 76% of the events were generated under counter-clockwise hysteresis (i.e., wet antecedent conditions), with 48% occurring in winter. 7% of events occurred under dry conditions, with clockwise hysteresis; and the rest of the floods (17%) had a complex hysteresis pattern (Table 4). The largest R and SL contribution performed counter-clockwise (R: 50%, SL: 36%) and complex (R: 50%, SL: 61%) hysteresis (Table 4).

To assess the highest R and SL contributions with the Q-SSC and SM-Q hysteresis types, the R and SL contributions by hysteresis type

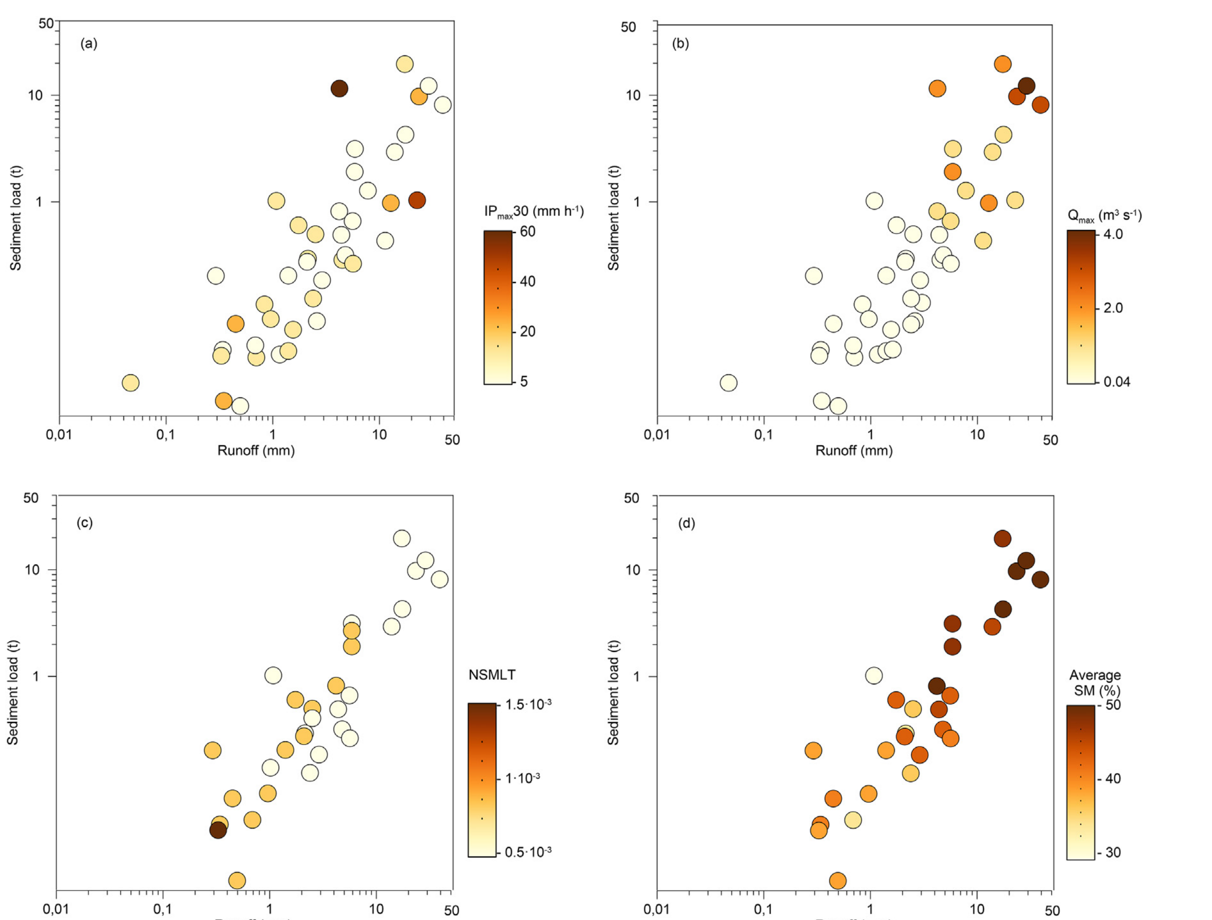

Fig. 4. Relationship between runoff and sediment load at the event scale in light of a third variable represented as a colour scale: (a) $IP_{max}30$, (b) Q_{max}, (c) NSMLT, (d) SM_{av}.

Table 4
Percentage of hysteresis types, in the event scale discharge-SSC and soil moisture-discharge relationships. Percentage of runoff by hysteresis type for discharge-suspended sediment concentration and soil moisture-discharge relationships. Percentage of sediment load by hysteresis type for discharge-suspended sediment concentration and soil moisture-discharge relationships.

	Hysteresis shape	Hysteresis type (%)	Runoff yield by hysteresis type (%)	Sediment load by hysteresis type (%)
Discharge - SSC hysteresis	Linear	15.6	6.5	4.3
	Clockwise	57.8	56.8	52.2
	Counter-clockwise	17.8	18.4	30.5
	Complex	8.9	18.3	13.1
Soil moisture - discharge hysteresis	Clockwise	6.9	0.7	0.2
	Counter-clockwise	75.9	49.6	38.5
	Complex	17.2	49.7	61.3

(Table 4) were compared to these events with the highest contributions (i.e., events with NSMLT < Q50 and SM_{av} > Q50). Accumulated R and SL in events with NSMLT < Q50 were 74% and 75%, respectively. Such values increased to 91% (R) and 96% (SL) in events with SM_{av} > Q50. In addition, the hysteresis type of both groups coincided with the main observed hysteretic pattern (Table 4), as clockwise (57% in NSMLT < Q50, 53% in SM_{av} > Q50) and counter-clockwise (67% in NSMLT < Q50, 64% in SM_{av} > Q50) patterns were predominant in the Q-SSC and SM-Q relationships, respectively. In addition, R and SL contributions by hysteresis type also coincide between NSMLT < Q50, SM_{av} > Q50 and the general pattern observed (Table 4).

The hydrological and sediment responses observed during the 5 flood events with the highest SL contribution (Fig. 5) covered a wide range of P (44–115 mm) and R (4–39 mm) depths. The event that occurred in September 2014 was characterized by the highest P intensity ($IP_{max}30 = 56$ mm h^{-1}), the highest SSC (2800 mg l^{-1}) and the lowest R out of all the selected events (Fig. 5a). The other events (Fig. 5b to e) occurred between late December and early February, the period with the lowest evapotranspiration. Although a wide range of P can be seen, R and Q_{max} values were always higher than 20 mm and 2 m^3 s^{-1}, respectively. These flood events were characterized by similar hydrograph shapes (i.e., long recession), SM_{av} > 45%, counter-clockwise or complex SM-Q hysteretic behaviour, and in all cases, soil saturation (i.e., the green line in Fig. 5). However, similar P (44 mm) and SL (12 t) amounts can be seen in events occurring in different seasons and under different SM conditions (Fig. 5a and e). For Q-SSC hysteresis, counter-clockwise hysteresis was associated with the highest values of SSC (Fig. 5a and b), whereas SSC values were <300 mg l^{-1} for clockwise hysteresis.

5. Discussion

The role of SM in R and SL dynamics at the catchment scale is determined by initial moisture conditions in temperate, arctic, alpine and Mediterranean catchments (Seeger et al., 2004; Penna et al., 2011; Favaro and Lamoureux, 2014; Rodríguez-Blanco et al., 2019). Nonetheless, the highly marked seasonality of the Mediterranean climate is a key factor controlling hydrological processes and sediment transport (Lana-Renault and Regüés, 2009), as evapotranspiration determines a succession of different hydrological seasons during the year (Gallart et al., 2002). Accordingly, assessing event seasonality in the P-SM-R-SL relationships is crucial to the understanding of SL variability (Regüés and Gallart, 2004).

5.1. Inter- and intra-annual variability of water and sediment yield

High variations in annual R and SY in Mediterranean catchments were due to the inter- and intra-annual variability of the P amount,

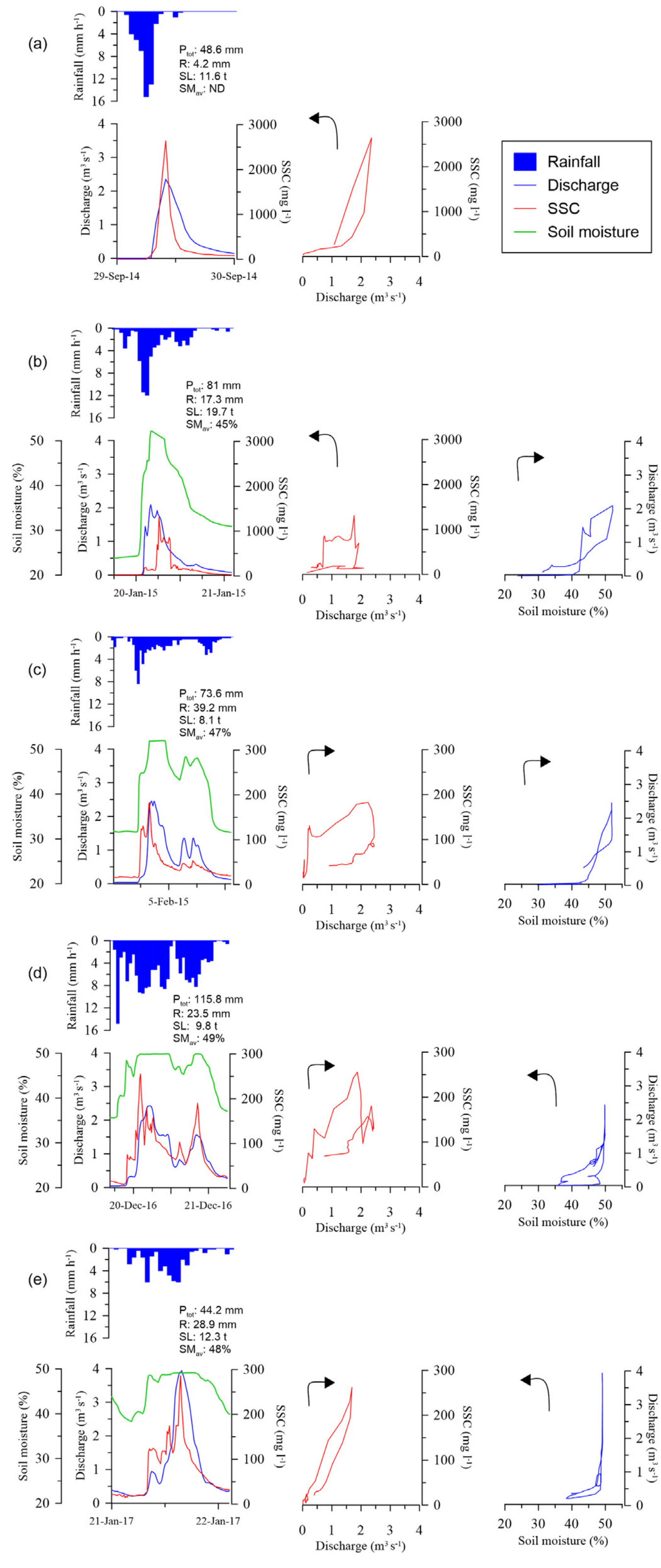

Fig. 5. Rainfall, soil moisture, discharge and suspended sediment concentration for the five largest events in terms of sediment load contribution. Discharge-suspended sediment concentration and soil moisture-discharge hysteresis for each event are also shown.

which generated seasonal patterns of R and SY (Bonada and Resh, 2013; Smetanová et al., 2018; Fortesa et al., 2020a). Thus, short datasets can lead to under- or over-estimates (García-Ruiz et al., 2015). To record events of low frequency and high magnitude, medium (i.e., 5 years) and long-term (i.e., 10–20 years) representative databases are needed (Nadal-Romero et al., 2018; Esteves et al., 2019).

In this study, five hydrological years (i.e., dry, average and wet years) were studied to assess the role of SM in R and SS transport in a mid-mountain Mediterranean catchment. Inter-annual variability in the annual SY ranged from <0.1 to 11.9 t km^2 yr^{-1} with an average of 5.4 t km^2 yr^{-1}. These values are very low when compared with the SY reported in European catchments by Vanmaercke et al. (2011). Es Fangar can be classified in the catchment group with lowest SY (i.e., <40 t km^2 yr^{-1}). Es Fangar SY is comparable with other Mediterranean catchments with similar characteristics in terms of catchment area and climate, with their SY ranging from 0.1 to 14 t km^2 yr^{-1} (Sala and Farguell, 2002; Estrany et al., 2009; Pacheco et al., 2011; Calsamiglia et al., 2016; García-Comendador et al., 2017; López-Tarazón and Estrany, 2017). The low values of SY can be explained by the spatial distribution of the physical driving factors (lithology and land cover), human structures (terraces) and land cover changes in the catchment. Since 1950, farmland abandonment of marginal areas and subsequent afforestation increased rainfall interception and transpiration by shrubs and forests (Keesstra et al., 2009; Lana-Renault et al., 2020). These changes, i.e. when agriculture uses are displaced by forests, trigger a reduction in R and SL amounts (García-Ruiz, 2010; Buendia et al., 2016a,b). Accordingly, cleaner water flowing from middle-upper forest parts of Mediterranean mountainous catchments was measured (Nadal-Romero et al., 2008a). The spatial distribution of land uses in Es Fangar follows a common landscape pattern in Mediterranean regions; i.e., forests at headwaters and agriculture in the valley bottom. This land use distribution promotes a reduction effect in R and SS response, as the steepest parts of the catchments are covered by natural vegetation. Furthermore, carbonate materials and karst features led to lower R and SS transport values due to higher infiltration rates and lower SS availability than marls and schists did (Cantón et al., 2011; Li et al., 2019). Low SS availability is related to the low soil formation observed in karst areas (i.e., 0.2–55 t km^{-2} y^{-1}; Cao et al., 2020), when compared to the average rate of soil formation in Europe (140 t km^{-2} y^{-1}, Verheijen et al., 2009). In Es Fangar, the middle and upper parts of the catchment are dominated by these carbonate materials and karst features (i.e., 44% of the catchment area). Marl materials are located in areas with the lowest gradient slopes of the catchment but with agricultural uses. Hence, the highest SS availability is developed in agricultural soils in the middle and lower parts of the catchment. In addition, in the more erodible areas within the agriculture fields, check-dams and terraces were built, which avoided rill erosion, laminated R and retained soil (Tarolli et al., 2014). In addition, subsurface tile drains in flat areas facilitated drainage during wet periods by reducing soil saturation (Estrany et al., 2010). However, the abandonment and collapse of these structures may lead to increased R and sediment pathways, as terraces are a potential source of sediment (Calsamiglia et al., 2018, 2020).

Intra-annual SL variability can be seen better when major SS transport takes place. In Es Fangar, 80% of the SL occurred in the autumn and winter seasons, which were characterized by a higher soil moisture interquartile range than spring and summer were. Similar dynamics were observed in Mediterranean catchments, obtaining SL contributions ranging from 71% to 98% during the wet season (Estrany et al., 2009; Taguas et al., 2013). That the highest amounts of SL occurred during the wet season is a pattern of Mediterranean catchments (Smetanová et al., 2018). Although during dry periods flood events occur less frequently in Mediterranean catchments (Merheb et al., 2016), when they do occur they are usually caused by high rainfall intensities in a flashy form at the end of summer (Gaume et al., 2009). These events move high amounts of SL in a short time period, as occurred at Es Fangar at the end of the hydrological year 2013–14 (77% of the annual yield in 0.5% of the time).

5.2. Event scale

5.2.1. Hydro-sedimentary response on the event scale

The sediment supply of a river follows a non-linear pattern. Thus, few events are responsible for the main loads, as between 80% and 90% of the SS load is transported between 1% and 12% of the time in both humid catchments (Zabaleta et al., 2007; Rodríguez-Blanco et al., 2019) and Mediterranean ones (Rovira and Batalla, 2006; Estrany et al., 2009; López-Tarazón et al., 2009). The same behaviour was seen at Es Fangar, where 91% of the SL was transported in 5% of the time.

The identification of SL driving factors can be explored through its relationship with P, R, Q_{max} and SM_{av}. The rainfall depth was not a good SL predictor, as is seen in the R generation in Es Fangar and other small Mediterranean catchments (Nadal-Romero et al., 2018). However, flood events characterized by high values of R and Q_{max} do transport the largest amounts of SL (López-Tarazón and Estrany, 2017; Licciardello et al., 2019). Accordingly, in Es Fangar the variance explained in the R-SL (67%) and Q_{max}-SL (86%) relationships obtained the highest values. The same key role was clarified by R and Q_{max} in the SL, explaining 70% and 68% of the variance, respectively, in a humid Mediterranean badland catchment (Nadal-Romero et al., 2008a). However, R-SL and Q_{max}-SL correlations increased during dry periods (up to 92% variance) in Nadal-Romero et al. (2008a), but in Es Fangar they increased (up to 89% variance) during the autumn and winter periods. In Es Fangar, this pattern is promoted by the favourable conditions of soil moisture during the wet period. Consequently, the explained variance in the annual average SM_{av}-SL relationship (45%) increased to 77% and 75% in autumn and winter seasons, respectively. Consequently, seasonality plays a key role in soil moisture conditions and, thus, in R generation (Lana-Renault et al., 2007) and SL contribution, causing the highest R and SL contributions (Nadal-Romero et al., 2008a). At Es Fangar, autumn and winter relationships between SL and R, Q_{max} and SM_{av} explained 72% to 89% of the SL variance. On the contrary, rainfall intensity was not mainly related to R and SL generation; i.e., $IP_{max}30$ did not show correlation with SL, except in one event characterized by high rainfall intensity (56 mm h^{-1}), large Q_{max} (2.4 m^3 s^{-1}) and the greatest SSC_{max} (2641 mg l^{-1}), which generated a SL of 11.6 t. It is clear that this type of event was infrequent and only occurred during the dry period, as the infiltration excess processes were dominant due to high rainfall intensities (Nadal-Romero et al., 2016).

The R-SL relationship combined with Q_{max}, NSMLT and SM_{av} showed how the highest SL contributions were generated when flood events occurred in autumn or winter, $R > 5$ mm, $Q_{max} > 0.8$ m^3 s^{-1}, $SM_{av} > 45\%$ and NSMLT < Q50. The largest values of R and Q_{max} generated the highest values of SL because the values of R and Q_{max} were promoted by favourable SM antecedent conditions and seasonality (8 out of 9 events occurred in autumn and winter) (Nadal-Romero et al., 2018). It should be noted that events under wet conditions triggered shorter travel time and lag time between the beginning of the rainfall event and the water table peak than events under dry conditions (Penna et al., 2011; van Meerveld et al., 2019). At Es Fangar, events with NSMLT < Q50 had higher R, Q_{max} and SL values than NSMLT > Q50, with bigger contributions since catchment moisture was greater due to an expansion of the wet stream length (Jensen et al., 2019). Situations of high catchment connectivity occurred during the window of soil moisture, promoting large R and SL contributions due to moist or saturated soil. On the contrary, events out of the soil moisture window tended to have smaller R and SL contributions because they occurred when soil was less moist or relatively dry (Gómez et al., 2014).

5.2.2. Hysteretic patterns

Different sediment sources were probably activated according in line with the changing hysteresis patterns of Q-SSC. Clockwise was the most frequent hysteresis pattern, especially during the wet season, because lower rainfall intensities and higher vegetation cover reduced sediment availability on catchment slopes, hindering bank erosion, mobilization and depletion of in-channel sediment or nearby sediment sources (Gellis, 2013) during low to medium-magnitude flood events. This clockwise hysteresis is common in the wet season in Mediterranean catchments (e.g., Seeger et al., 2004; Rovira and Batalla, 2006; Soler et al., 2008; Giménez et al., 2012; López-Tarazón and Estrany, 2017). Assessing hysteresis behaviour in small catchments is an approach that may improve understanding of sediment connectivity, as substantial knowledge of small catchments exists in other studies (Keesstra et al., 2019). The higher frequency and SL volume of clockwise Q-SSC hysteresis confirm that SS in Es Fangar is mostly generated from sources that are relatively close to the main channel system; i.e., agricultural fields over marl materials where there is the highest SS availability.

At Es Fangar the combined effect of afforestation, soil conservation structures and limestone lithology caused low sediment availability and connectivity due to rainfall interception, sediment retention and deep percolation, as has also been seen in other Mediterranean and non-Mediterranean catchments (Haddadchi and Hicks, 2019; Calsamiglia et al., 2020; Poeppl et al., 2020). Clockwise and linear hysteresis (i.e., 73% of hysteresis and 57% of SL) occurred due to sediment released from nearby areas. That is, sediment generated within bed-channel and agricultural fields activated a rapid SSC increase at the beginning of the flood and decreased before the discharge peak, suggesting rapid sediment exhaustion (Regüés and Gallart, 2004). In addition, the clockwise loop pattern was the most common hysteresis type in small headwater catchments because flowpaths from the source areas of the sediment are short (Nadal-Romero et al., 2008b; Aich et al., 2014).

A counter-clockwise pattern was observed in Mediterranean catchments with highly erodible materials (Nadal-Romero et al., 2008b; Soler et al., 2008; Tuset et al., 2016), in multi-peak events (De Girolamo et al., 2015) and in a large catchment when the rainfall event is located at the headwaters (López-Tarazón et al., 2009). However, in Es Fangar counter-clockwise loops occurred between late autumn and early spring when water reserves were high. These loops were generated in the wet period when hydrological pathways were active due to high or saturated moisture conditions; i.e., allowing a more continuous sediment transfer which would not be available with less moisture conditions (Seeger et al., 2004).

Figure-eight hysteresis was observed during transition periods (Soler et al., 2008) and in multiple peak events occurring during wet periods (Nadal-Romero et al., 2008b). At Es Fangar, similarly to counter-clockwise shapes, the figure-eight was observed during late autumn and winter, being common under runoff coefficients >20%. The low frequency of counter-clockwise (18%) and figure-eight (9%) hysteresis indicates that antecedent wet conditions in some flood events activated of hydrological pathways and consequently new sediment-contributing areas (Seeger et al., 2004). As a result, these hysteresis shapes were related to both 37% of R and 44% of SL. In a very similar way, 76% and 17% of the twenty-eight flood events used for analysing SM-Q hysteresis were, respectively, counter-clockwise and complex in shape. These hysteresis types were related to 99% of R and SL during these 28 selected events, highlighting again the significant role of wet antecedent conditions (Penna et al., 2011).

6. Conclusions

The assessment of soil moisture, runoff and sediment load dynamics at different temporal scales improved understanding of erosion processes in a mid-mountain small Mediterranean catchment. At the annual scale, low values of runoff and sediment load were related to limestone lithology, afforested hillslopes and soil conservation structures. Large inter-annual variability was observed, with sediment yields in three different orders of magnitude (0.08 to 11.86 t km^{-2} y^{-1}). Intra-annual variability showed how 80% of sediment load was generated during the wet period and in short period of time.

At the event scale, soil moisture significantly affected the hydrological processes in Es Fangar, but mainly during wet periods, when the highest values of runoff, peak discharge and sediment load occurred. In addition, 73% of sediment load was generated in five of the 45 events, with precipitation being a poor predictor. Runoff and peak discharge showed the closest correlations with sediment load, correlations that increased in autumn and winter.

The highest frequency of clockwise hysteresis in the discharge-suspended sediment concentration relationship showed that the main suspended sediment sources were close to the catchment outlet, as there was limited sediment availability. Although counter-clockwise patterns were less frequent, their occurrence was linked to the wet period (i.e., high moisture content), when the hydrological connectivity of the catchment was higher and less available sediment sources could be activated. The soil moisture-discharge hysteresis analysis confirmed that 76% of flood events were generated under wet antecedent conditions (i.e., 48% in winter), responsible for the highest amount of runoff and sediment load.

Considering the complexity and spatial variability of Mediterranean catchments, case studies are useful to improve the understanding of SL contributions through SM assessment. Further studies analysing the role of soil moisture in SL dynamics in representative small catchments under different lithology and land use will deepen our grasp of this relationship.

Declaration of competing interest

The authors declare that they have no known competing financial interests or personal relationships that could have appeared to influence the work reported in this paper.

Acknowledgments

This research was supported by project CGL2017-88200-R “Functional hydrological and sediment connectivity at Mediterranean catchments: global change scenarios –MEDhyCON2”, funded by the Spanish Ministry of Science, Innovation and Universities, the Spanish Agency of Research (AEI) and the European Regional Development Fund (ERDF). The contribution of Jérôme Latron was supported by the research project PCIN-2017-061/AEI, also funded by the Spanish Government. Josep Fortesa has a contract funded by the Ministry of Innovation, Research and Tourism of the Autonomous Government of the Balearic Islands [FPI/2048/2017]. Julián García-Comendador is in receipt of a pre-doctoral contract [FPU15/05239] funded by the Spanish Ministry of Education, Culture and Sports. Jaume Company is in receipt of a Young Qualified Program funded by the Employment Service of the Balearic Islands and European Social Fund (SJ-QSP 48/19). Some of the meteorological data were provided by the Spanish Meteorological Agency (AEMET).

Appendix A

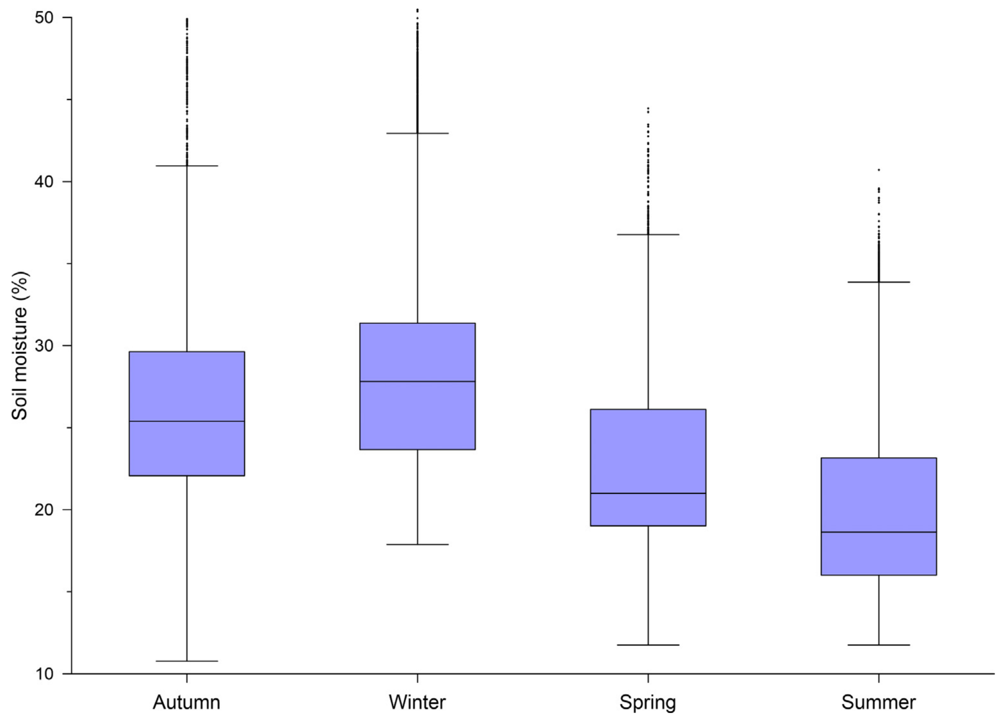

Fig. 1. Quartile values of seasonal soil moisture recorded in 15-min steps during the hydrological years 2012–2017. Outliers are shown as black dots.

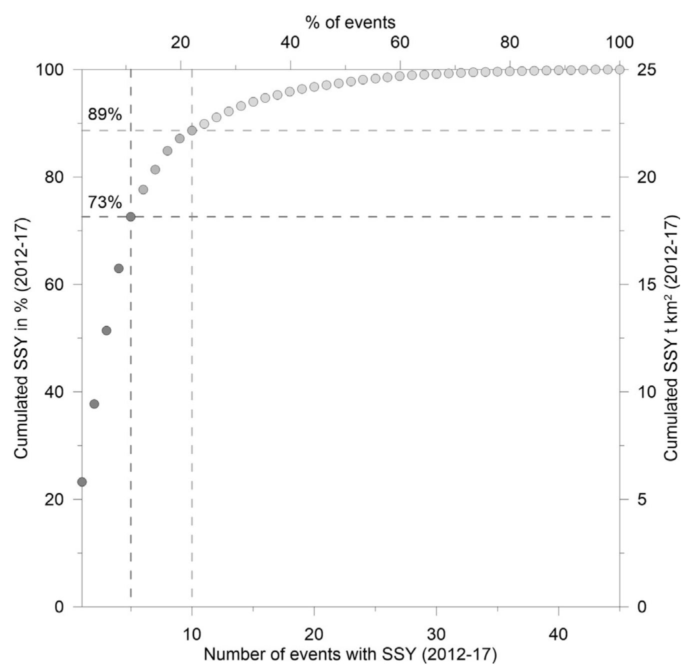

Fig. 2. Number of events in absolute and relative values with suspended sediment yield data during the hydrological years 2012–2017. The Y axis shows the accumulated suspended sediment yield in absolute and relative values.

References

Aich, V., Zimmermann, A., Elsenbeer, H., 2014. Quantification and interpretation of suspended-sediment discharge hysteresis patterns: how much data do we need? Catena 122, 120–129. https://doi.org/10.1016/J.CATENA.2014.06.020.

Bonada, N., Resh, V.H., 2013. Mediterranean-climate streams and rivers: geographically separated but ecologically comparable freshwater systems. Hydrobiologia. https://doi.org/10.1007/s10750-013-1634-2.

Brocca, L., Melone, F., Moramarco, T., Morbidelli, R., 2010. Spatial-temporal variability of soil moisture and its estimation across scales. Water Resour. Res. 46. https://doi.org/10.1029/2009WR008016.

Buendia, C., Batalla, R.J., Sabater, S., Palau, A., Marcé, R., 2016a. Runoff trends driven by climate and afforestation in a Pyrenean Basin. L. Degrad. Dev. 27, 823–838. https://doi.org/10.1002/ldr.2384.

Buendia, C., Bussi, G., Tuset, J., Vericat, D., Sabater, S., Palau, A., Batalla, R.J., 2016b. Effects of afforestation on runoff and sediment load in an upland Mediterranean catchment. Sci. Total Environ. 540, 144–157. https://doi.org/10.1016/j.scitotenv.2015.07.005.

Bussi, G., Francés, F., Horel, E., López-Tarazón, J.A., Batalla, R.J., 2014. Modelling the impact of climate change on sediment yield in a highly erodible Mediterranean catchment. J. Soils Sediments 14, 1921–1937. https://doi.org/10.1007/s11368-014-0956-7.

Calsamiglia, A., Fortesa, J., Garcia-Comendador, J., Estrany, J., 2016. Respuesta hidrosedimentaria en dos cuencas mediterráneas representativas afectadas por el cambio global. Cuaternario y Geomorfol. 30, 87–103. doi:10.17735/cyg.v30i1-2.45900.

Calsamiglia, A., Fortesa, J., García-Comendador, J., Lucas-Borja, M.E., Calvo-Cases, A., Estrany, J., 2018. Spatial patterns of sediment connectivity in terraced lands: anthropogenic controls of catchment sensitivity. L. Degrad. Dev. 29, 1198–1210. https://doi.org/10.1002/ldr.2840.

Calsamiglia, A., Gago, J., García-Comendador, J., Fortesa, J., Calvo-Cases, A., Estrany, J., 2020. Evaluating functional connectivity in a small agricultural catchment under contrasting flood events by using UAV. Earth Surf. Process. Landforms, esp.4769 https://doi.org/10.1002/esp.4769.

Cantón, Y., Solé-Benet, A., De Vente, J., Boix-Fayos, C., Calvo-Cases, A., Asensio, C., Puigdefábregas, J., 2011. A review of runoff generation and soil erosion across scales in semiarid south-eastern Spain. J. Arid Environ. 75, 1254–1261. https://doi.org/10.1016/j.jaridenv.2011.03.004.

Cao, L., Wang, S., Peng, T., Cheng, Q., Zhang, L., Zhang, Z., Yue, F., Fryer, A.E., 2020. Monitoring of suspended sediment load and transport in an agroforestry watershed on a karst plateau, Southwest China. Agric. Ecosyst. Environ. 299, 106976. https://doi.org/10.1016/j.agee.2020.106976.

De Girolamo, A.M., Pappagallo, G., Lo Porto, A., 2015. Temporal variability of suspended sediment transport and rating curves in a Mediterranean river basin: the Celone (SE Italy). Catena 128, 135–143. https://doi.org/10.1016/j.catena.2014.09.020.

Esteves, M., Legout, C., Navratil, O., Evrard, O., 2019. Medium term high frequency observation of discharges and suspended sediment in a Mediterranean mountainous catchment. J. Hydrol. 568, 562–574. https://doi.org/10.1016/j.jhydrol.2018.10.066.

Estrany, J., Garcia, C., Batalla, R.J., 2009. Suspended sediment transport in a small Mediterranean agricultural catchment. Earth Surf. Process. Landforms 34, 929–940. https://doi.org/10.1002/esp.1777.

Estrany, J., Garcia, C., Batalla, R.J., 2010. Hydrological response of a small Mediterranean agricultural catchment. J. Hydrol. 380, 180–190. https://doi.org/10.1016/j.jhydrol.2009.10.035.

Favaro, E.A., Lamoureux, S.F., 2014. Antecedent Controls on Rainfall Runoff Response and Sediment Transport in a High Arctic Catchment. Geogr. Ann. Ser. A, Phys. Geogr. 96, n/a-n/a. doi:https://doi.org/10.1111/geoa.12063.

Fortesa, J., Latron, J., García-Comendador, J., Tomàs-Burguera, M., Company, J., Calsamiglia, A., Estrany, J., 2020a. Multiple temporal scales assessment in the hydrological response of small Mediterranean-climate catchments. Water 12, 299. https://doi.org/10.3390/w12010299.

Fortesa, J., Ricci, G.F., García-Comendador, J., Gentile, F., Estrany, J., Sauquet, E., Datry, T., De Girolamo, A.M., 2020. Analysing hydrological and sediment transport regime in two Mediterranean intermittent rivers. Catena (Submitted for publication).

Gallart, F., Llorens, P., Latron, J., Regüés, D., 2002. Hydrological processes and their seasonal controls in a small Mediterranean mountain catchment in the Pyrenees. Hydrol. Earth Syst. Sci. 6, 527–537. https://doi.org/10.5194/hess-6-527-2002.

García-Comendador, J., Fortesa, J., Calsamiglia, A., Calvo-Cases, A., Estrany, J., 2017. Post-fire hydrological response and suspended sediment transport of a terraced Mediterranean catchment. Earth Surf. Process. Landforms 42, 2254–2265. https://doi.org/10.1002/esp.4181.

García-Ruiz, J.M., 2010. The effects of land uses on soil erosion in Spain: a review. Catena https://doi.org/10.1016/j.catena.2010.01.001.

García-Ruiz, J.M., Beguería, S., Nadal-Romero, E., González-Hidalgo, J.C., Lana-Renault, N., Sanjuán, Y., 2015. A meta-analysis of soil erosion rates across the world. Geomorphology. https://doi.org/10.1016/j.geomorph.2015.03.008.

Gaume, E., Bain, V., Bernardara, P., Newinger, O., Barbuc, M., Bateman, A., Blaškovičová, L., Blöschl, G., Borga, M., Dumitrescu, A., Daliakopoulos, I., Garcia, J., Irimescu, A., Kohnova, S., Koutroulis, A., Marchi, L., Matreata, S., Medina, V., Preciso, E., Sempere-Torres, D., Stancalie, G., Szolgay, J., Tsanis, I., Velasco, D., Viglione, A., 2009. A compilation of data on European flash floods. J. Hydrol. 367, 70–78. https://doi.org/10.1016/J.JHYDROL.2008.12.028.

Geeson, N., Brandt, C.J., Thornes, J.B., 2002. Mediterranean Desertification: A Mosaic of Processes and Responses. John Wiley & Sons.

Gellis, A.C., 2013. Factors influencing storm-generated suspended-sediment concentrations and loads in four basins of contrasting land use, humid-tropical Puerto Rico. Catena 104, 39–57. https://doi.org/10.1016/j.catena.2012.10.018.

Giménez, R., Casalí, J., Grande, I., Díez, J., Campo, M.A., Álvarez-Mozos, J., Goñi, M., 2012. Factors controlling sediment export in a small agricultural watershed in Navarre (Spain). Agric. Water Manag. 110, 1–8. https://doi.org/10.1016/J.AGWAT.2012.03.007.

Gómez, J.A., Vanwalleghem, T., De Hoces, A., Taguas, E.V., 2014. Hydrological and erosive response of a small catchment under olive cultivation in a vertic soil during a five-year period: implications for sustainability. Agric. Ecosyst. Environ. 188, 229–244. https://doi.org/10.1016/j.agee.2014.02.032.

Guijarro, J.A., 1986. Contribución a la Bioclimatología de Baleares. Universitat de les Illes Balears.

Haddadchi, A., Hicks, M., 2019. Understanding the effect of catchment characteristics on suspended sediment dynamics during flood events. Hydrol. Process. Hyp., 13682 https://doi.org/10.1002/hyp.13682.

Hooke, J.M., 2006. Human impacts on fluvial systems in the Mediterranean region. Geomorphology 79, 311–335. https://doi.org/10.1016/j.geomorph.2006.06.036.

Huza, J., Teuling, A.J., Braud, I., Grazioli, J., Melsen, L.A., Nord, G., Raupach, T.H., Uijlenhoet, R., 2014. Precipitation, soil moisture and runoff variability in a small river catchment (Ardèche, France) during HyMeX Special Observation Period 1. J. Hydrol. 516, 330–342. https://doi.org/10.1016/j.jhydrol.2014.01.041.

Jaeger, K.L., Sutfin, N.A., Tooth, S., Michaelides, K., Singer, M., 2017. Geomorphology and sediment regimes of intermittent rivers and ephemeral streams. Intermittent Rivers Ephemer. Streams, 21–49 https://doi.org/10.1016/B978-0-12-803835-2.00002-4.

Jensen, C.K., McGuire, K.J., McLaughlin, D.L., Scott, D.T., 2019. Quantifying spatiotemporal variation in headwater stream length using flow intermittency sensors. Environ. Monit. Assess. 191. https://doi.org/10.1007/s10661-019-7373-8.

Keesstra, S.D., van Dam, O., Verstraeten, G., van Huissteden, J., 2009. Changing sediment dynamics due to natural reforestation in the Dragonja catchment, SW Slovenia. Catena 78, 60–71. https://doi.org/10.1016/j.catena.2009.02.021.

Keesstra, S.D., Davis, J., Masselink, R.H., Casalí, J., Peeters, E.T.H.M., Dijksma, R., 2019. Coupling hysteresis analysis with sediment and hydrological connectivity in three agricultural catchments in Navarre, Spain. J. Soils Sediments 19, 1598–1612. https://doi.org/10.1007/s11368-018-02223-0.

Kirkby, M., 2005. Organization and Process. Encyclopedia of Hydrological Sciences. John Wiley & Sons, Ltd, Chichester, UK. https://doi.org/10.1002/0470848944.hsa003.

Korres, W., Reichenau, T.G., Fiener, P., Koyama, C.N., Bogena, H.R., Cornelissen, T., Baatz, R., Herbst, M., Diekkrüger, B., Vereecken, H., Schneider, K., 2015. Spatio-temporal soil moisture patterns - a meta-analysis using plot to catchment scale data. J. Hydrol. 520, 326–341. https://doi.org/10.1016/j.jhydrol.2014.11.042.

Lana-Renault, N., Regüés, D., 2009. Seasonal patterns of suspended sediment transport in an abandoned farmland catchment in the Central Spanish Pyrenees. Earth Surf. Process. Landforms 34, 1291–1301. https://doi.org/10.1002/esp.1825.

Lana-Renault, N., Latron, J., Regüés, D., 2007. Streamflow response and water-table dynamics in a sub-Mediterranean research catchment (Central Pyrenees). J. Hydrol. 347, 497–507. https://doi.org/10.1016/J.JHYDROL.2007.09.037.

Lana-Renault, N., Nadal-Romero, E., Cammeraat, E., Llorente, J.Á., 2020. Critical environmental issues confirm the relevance of abandoned agricultural land. Water (Switzerland) https://doi.org/10.3390/W12041119.

Li, Z., Xu, X., Zhu, J., Xu, C., Wang, K., 2019. Effects of lithology and geomorphology on sediment yield in karst mountainous catchments. Geomorphology 343, 119–128. https://doi.org/10.1016/j.geomorph.2019.07.001.

Licciardello, F., Barbagallo, S., Gallart, F., 2019. Hydrological and erosional response of a small catchment in Sicily. J. Hydrol. Hydromech 67, 201–212. https://doi.org/10.2478/johh-2019-0003.

López-Tarazón, J.A., Estrany, J., 2017. Exploring suspended sediment delivery dynamics of two Mediterranean nested catchments. Hydrol. Process. 31, 698–715. https://doi.org/10.1002/hyp.11069.

López-Tarazón, J.A., Batalla, R.J., Vericat, D., Francke, T., 2009. Suspended sediment transport in a highly erodible catchment: the River Isábena (Southern Pyrenees). Geomorphology 109, 210–221. https://doi.org/10.1016/j.geomorph.2009.03.003.

Merheb, M., Moussa, R., Abdallah, C., Colin, F., Perrin, C., Baghdadi, N., 2016. Hydrological response characteristics of Mediterranean catchments at different time scales: a meta-analysis. Hydrol. Sci. J. 61, 2520–2539. https://doi.org/10.1080/02626667.2016.1140174.

Nadal-Romero, E., Cammeraat, E., Serrano-Muela, M.P., Lana-Renault, N., Regüés, D., 2016. Hydrological response of an afforested catchment in a Mediterranean humid mountain area: a comparative study with a natural forest. Hydrol. Process. 30, 2717–2733. https://doi.org/10.1002/hyp.10820.

Nadal-Romero, E., Latron, J., Martí-Bono, C., Regüés, D., 2008a. Temporal distribution of suspended sediment transport in a humid Mediterranean badland area: the Araguás catchment, Central Pyrenees. Geomorphology 97, 601–616. https://doi.org/10.1016/j.geomorph.2007.09.009.

Nadal-Romero, E., Regüés, D., Latron, J., 2008b. Relationships among rainfall, runoff, and suspended sediment in a small catchment with badlands. Catena 74, 127–136. https://doi.org/10.1016/j.catena.2008.03.014.

Nadal-Romero, E., Peña-Angulo, D., Regüés, D., 2018. Rainfall, run-off, and sediment transport dynamics in a humid mountain badland area: long-term results from a small catchment. Hydrol. Process. 32, 1588–1606. https://doi.org/10.1002/hyp.11495.

Oueslati, O., De Girolamo, A.M., Abouabdillah, A., Kjeldsen, T.R., Lo Porto, A., 2015. Classifying the flow regimes of Mediterranean streams using multivariate analysis. Hydrol. Process. 29, 4666–4682. https://doi.org/10.1002/hyp.10530.

Pacheco, E., Farguell, J., Úbeda, X., Outeiro, L., Miguel, A., 2011. Runoff and sediment producti on in a mediterranean basin under two diff erent land uses. Cuaternario y Geomorfol. 25, 103–114.

Palleiro, L., Rodríguez-Blanco, M.L., Taboada-Castro, M.M., Taboada-Castro, M.T., 2014. Hydroclimatic control of sediment and metal export from a rural catchment in northwestern Spain. Hydrol. Earth Syst. Sci. 18, 3663–3673. https://doi.org/10.5194/hess-18-3663-2014.

Penna, D., Tromp-Van Meerveld, H.J., Gobbi, A., Borga, M., Dalla Fontana, G., 2011. The influence of soil moisture on threshold runoff generation processes in an alpine headwater catchment. Hydrol. Earth Syst. Sci. 15, 689–702. https://doi.org/10.5194/hess-15-689-2011.

Poeppl, R.E., Fryirs, K.A., Tunnicliffe, J., Brierley, G.J., 2020. Managing sediment (dis)connectivity in fluvial systems. Sci. Total Environ. 736, 139627. https://doi.org/10.1016/j.scitotenv.2020.139627.

Pulley, S., Collins, A.L., 2019. Field-based determination of controls on runoff and fine sediment generation from lowland grazing livestock fields. J. Environ. Manag. 249, 109365. https://doi.org/10.1016/J.JENVMAN.2019.109365.

Regüés, D., Gallart, F., 2004. Seasonal patterns of runoff and erosion responses to simulated rainfall in badland area in Mediterranean mountain conditions (Vallcebre, Southeastern Pyrenees). Earth Surf. Process. Landforms 29, 755–767. https://doi.org/10.1002/esp.1067.

Rodríguez-Blanco, M.L., Taboada-Castro, M.M., Taboada-Castro, M.T., 2019. An overview of patterns and dynamics of suspended sediment transport in an agroforest headwater system in humid climate: results from a long-term monitoring. Sci. Total Environ. 648, 33–43. https://doi.org/10.1016/J.SCITOTENV.2018.08.118.

Rovira, A., Batalla, R.J., 2006. Temporal distribution of suspended sediment transport in a Mediterranean basin: the Lower Tordera (NE SPAIN). Geomorphology 79, 58–71. https://doi.org/10.1016/j.geomorph.2005.09.016.

Sala, M., Farguell, J., 2002. Exportacion de agua y sedimento en dos pequeñas cuencas mediterraneas bajo diferentes usos del suelo. Sistema costero catalán. Cuaternario y Geomorfol. 16, 97–109.

Schick, P.A., 1967. Suspended sampler and bedload trap. Field methods for the study of slope and fluvial processes. Rev. Geomorphol. Dyn. 17, 181–182.

Seeger, M., Errea, M.-P.P., Beguería, S., Arnáez, J., Martí, C., García-Ruiz, J., Beguería, S., Arnáez, J., Martí, C., García-Ruiz, J.M., 2004. Catchment soil moisture and rainfall characteristics as determinant factors for discharge/suspended sediment hysteretic loops in a small headwater catchment in the Spanish Pyrenees. J. Hydrol. 288, 299–311. https://doi.org/10.1016/j.jhydrol.2003.10.012.

Smetanová, A., Le Bissonnais, Y., Raclot, D., Nunes, J.P., Licciardello, F., Le Bouteiller, C., Latron, J., Rodr Ig U, E., Caballero, E.Z., Mathys, N., Klotz, S., Mekki, I., Gallart, F., Sol E Benet, A., Er, N.P., Gallego, E.Z., Andrieux, P., Moussa, R., Planchon, O., Santos, J.M., Alshihabi, O., Chikhaoui, M., Follain, S., 2018. Temporal variability and time compression of sediment yield in small Mediterranean catchments: impacts for land and water management t. Soil Use Manag. 34, 388–403. https://doi.org/10.1111/sum.12437.

Soler, M., Latron, J., Gallart, F., 2008. Relationships between suspended sediment concentrations and discharge in two small research basins in a mountainous Mediterranean area (Vallcebre, Eastern Pyrenees). Geomorphology 98, 143–152. https://doi.org/10.1016/j.geomorph.2007.02.032.

Taguas, E.E.V., Ayuso, J.L.J., Pérez, R., Giráldez, J.V.J., Gómez, J.A.J., 2013. Intra and interannual variability of runoff and sediment yield of an olive micro-catchment with soil protection by natural ground cover in Southern Spain. Geoderma 206, 49–62. https://doi.org/10.1016/j.geoderma.2013.04.011.

Tarolli, P., Preti, F., Romano, N., 2014. Terraced landscapes: from an old best practice to a potential hazard for soil degradation due to land abandonment. Anthropocene. https://doi.org/10.1016/j.ancene.2014.03.002.

Tuset, J., Vericat, D., Batalla, R.J., 2016. Rainfall, runoff and sediment transport in a Mediterranean mountainous catchment. Sci. Total Environ. 540, 114–132. https://doi.org/10.1016/j.scitotenv.2015.07.075.

Uber, M., Vandervaere, J.-P., Zin, I., Braud, I., Heistermann, M., Legoût, C., Molinié, G., Nord, G., 2018. How does initial soil moisture influence the hydrological response? A case study from southern France. Hydrol. Earth Syst. Sci. 22, 6127–6146. https://doi.org/10.5194/hess-22-6127-2018.

van Meerveld, H.J.I., Kirchner, J.W., Vis, M.J.P., Assendelft, R.S., Seibert, J., 2019. Expansion and contraction of the flowing stream network alter hillslope flowpath lengths and the shape of the travel time distribution. Hydrol. Earth Syst. Sci. 23, 4825–4834. https://doi.org/10.5194/hess-23-4825-2019.

Vanmaercke, M., Poesen, J., Verstraeten, G., de Vente, J., Ocakoglu, F., 2011. Sediment yield in Europe: spatial patterns and scale dependency. Geomorphology 130, 142–161. https://doi.org/10.1016/J.GEOMORPH.2011.03.010.

Verheijen, F.G.A., Jones, R.J.A., Rickson, R.J., Smith, C.J., 2009. Tolerable versus actual soil erosion rates in Europe. Earth-Science Rev. https://doi.org/10.1016/j.earscirev.2009.02.003.

Williams, G., 1989. Sediment concentration versus water discharge during single hydrologic events in rivers. J. Hydrol. 111, 89–106.

YACU, 2002. Estudio de caracterización del régimen extremo de precipitaciones en la isla de Mallorca. Junta d'Aigües de les Illes Balears, Palma de Mallorca.

Zabaleta, A., Martínez, M., Uriarte, J.A., Antigüedad, I., 2007. Factors controlling suspended sediment yield during runoff events in small headwater catchments of the Basque Country. Catena 71, 179–190. https://doi.org/10.1016/j.catena.2006.06.007.

Zucco, G., Brocca, L., Moramarco, T., Morbidelli, R., 2014. Influence of land use on soil moisture spatial-temporal variability and monitoring. J. Hydrol. 516, 193–199. https://doi.org/10.1016/j.jhydrol.2014.01.043.